Interaction of dilute colloidal particles in a mixed solvent

M. L. Kurnaz and J. V. Maher

Department of Physics and Astronomy, University of Pittsburgh, Pittsburgh, Pennsylvania 15260

(Received 25 July 1994; revised manuscript received 6 March 1995)

We have measured the second virial coefficient B_2 of very dilute colloidal dispersions of charge-stabilized polystyrene latex spheres in the one-phase region of the mixed solvent 2,6-lutidine plus water. These measurements were made as a function of temperature for two solvent compositions, both of which are richer in 2,6-lutidine than the binary liquid mixture's critical composition. The temperature ranges started deep in the one-phase region and approached the coexistence curve but did not penetrate the region of reversible aggregation near the coexistence curve. Very large, positive (repulsive-interaction) virial coefficients are observed at temperatures far from the aggregation zone and for calibration samples whose solvent is pure water. These large values of B_2 are impossible to model without invoking long-range repulsive interactions whose origin is difficult to explain. As the temperature is brought nearer to the aggregation zone, the virial coefficient plunges through zero to large negative (attractive-interaction) values. Crude modeling suggests that the observed changes in the interactions are not inconsistent with a temperature-dependent attraction arising from adsorption layer energetics operating at distances of a few solvent-fluctuation correlation lengths from the particle surfaces.

PACS number(s): 68.45.Gd, 64.70.Ja, 78.35.+c, 82.70.Dd

I. INTRODUCTION

Recent experiments have shown that colloidal particles in mixed solvents can show reversible aggregation in the one-phase regime of the mixture near the mixture's phase separation temperature [1–5]. Most of these experiments have used 2,6-lutidine plus water (LW) as the mixed solvent and either silica or polystyrene latex spheres (PLS) as colloidal particles. In our work on PLS in LW [4,5], the aggregation condition has been shown to be related to the affinity of the colloidal surfaces for one of the solvent components. In particular, in a temperature range near the critical temperature, T_c, in the mixture's two-phase region, the particles will partition into one of the solvent phases, with the meniscus between the liquid phases clear to the eye and showing no sign of population by colloidal particles. Which phase of the solvent attracts the particles depends on the surface charge density of the particles, with high surface charge density particles preferring the water-rich phase and low charge density particles preferring the lutidine-rich phase. As temperature is advanced deeper into the two-phase region (all effects discussed here are equilibrium effects), there is a temperature T_w at which particles appear on the meniscus (most particles remain in the preferred phase, whose population depletion is too small to measure). T_w changes with the surface charge density of the particles [4], but not with radius or with number density of the particles in the sample. The aggregation observed in the one-phase region [5] is then restricted to the side of the solvent's coexistence curve poor in the component which is rich in the partitioning-favored phase.

While these phenomena are almost certainly related to the energetics of wetting-adsorption, we currently lack a complete understanding of the aggregation phenomenon, particularly since aggregation can occur both far into the solvent's one-phase region, distinctly beyond the critical temperature, and also along the side of the solvent coexistence curve far beyond the wetting temperature.

In this paper we present a measurement of the second virial coefficient for the interaction of very dilute colloidal particles deep in the one-phase region of the solvent, at temperatures ranging from very far from the point of onset of aggregation where the particle-particle interaction is clearly repulsive to near the temperature at which aggregation first appears.

II. EXPERIMENTAL DESIGN AND DATA ANALYSIS

As in our earlier work [4,5], the system studied was dilute suspensions of well-characterized, monodisperse [6] PLS in near-critical mixtures of 2,6-lutidine [7] plus water. PLS was prepared using a surfactant-free emulsion-polymerization technique, where stabilization against aggregation is provided by a net surface charge density of several $\mu C/cm^2$ from sulfonated end groups preferentially located on the surface of the sphere. (We use "surface charge density" as measured by titration as a measure of sulfonic groups available on the surface for solvation. The actual surface charge density should depend on the local solvent composition near the particle surface and has not been measured in this experiment.)

In our earlier work [4,5] we have measured the onset of the aggregation zone T_a. Figure 1 shows the results of those measurements for PLS particles of several surface charge densities, as well as the measured phase separation temperature T_{PS} at each of the solvent compositions used (at each point in Fig. 1 when the T_a and T_{PS} symbols
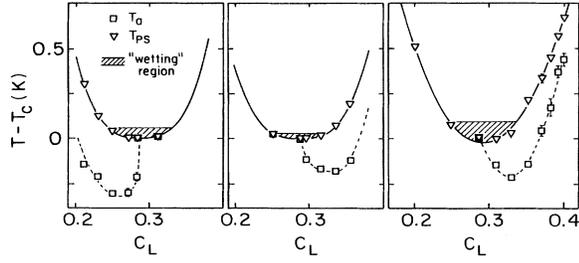
FIG. 1. Measured difference of phase separation temperature ($\bigtriangledown$) T_{PS} and aggregation temperature ($\square$) T_a from the critical temperature T_c vs solvent composition c_L. Also shown are the coexistence curve (solid line), the aggregation curve (dashed line, drawn to guide the eye), and expected complete wetting region (hashed region, from Ref. [9]). Particle types are left, $d = 0.371 \pm 0.02$ μm; $\sigma = 0.38$ μC/cm^2; middle, $d = 0.378 \pm 0.06$ μm, $\sigma = 3.85$ μC/cm^2; right, $d = 0.555 \pm 0.03$ μm, $\sigma = 5.70$ μC/cm^2.

overlap, no aggregation was observed). In this work we used dilute suspensions of PLS of diameter $d = 0.555$ μm (based on electron micrography) and surface charge density $\sigma = 5.70$ μC/cm^2 (as reported by the manufacturer), and thus the aggregation zone is as shown in Fig. 1(c).

Samples were made with a variety of colloidal-particle volume fraction ϕ $(2 \times 10^{-7} < \phi < 2 \times 10^{-4})$ and two different solvent compositions c_L $(c_L = 0.35$ and $c_L = 0.40)$. Static light scattering was measured as a function of wave number and number density of colloidal particles at each of a variety of temperatures $[(T_{\mathrm{coex}} - 4 \text{ K}) < T < T_a]$ for each of the two solvent compositions where T_{coex} is the coexistence temperature and T_a is the aggregation temperature for each LW composition. While identical aggregation behavior was observed over the full range of colloidal-particle number density, the most reliable light scattering results were obtained for colloid-particle volume fractions in the range $(3 \times 10^{-7} < \phi < 3 \times 10^{-6})$. Below this concentration the colloidal-particle light scattering signal becomes too weak for accurate separation from the solvent-fluctuation signal, and far above this concentration multiple scattering poses a problem. Accordingly the quantitative results presented below were all obtained in the range favorable to light scattering. In addition, measurements were made at one temperature for a series of samples of varying colloidal-particle density in pure water for purposes of calibration.

The colloidal-particle radius was chosen large enough that it was much larger than the correlation length for solvent fluctuations throughout the range of our measurements. It was then possible to subtract the essentially flat Lorentzian background scattering from solvent fluctuations and treat the remaining scattering as pure colloidal-particle scattering,

$$I_{\mathrm{ex}}(\theta) = I_s(\text{solution}) - I_s(\text{solvent}). \qquad (1)$$

This excess colloidal scattering $I_{\mathrm{ex}}(\theta)$ could then be written as

$$I_{\mathrm{ex}}(\theta) = NS(\theta)P(\theta), \qquad (2)$$

where $P(\theta)$ is the form factor for scattering of a beam of intensity I_0 from an isolated colloidal particle, $S(\theta)$ is the structure factor which carries all the information about correlations among colloidal particles, and N is the number density of colloidal particles.

For spherical particles of radius R [8],

$$P(\theta) = \frac{32\pi^4 R^6 |m^2 - 1|^2}{9\lambda^4 r^2} I_0 \frac{9(\sin x - x \cos x)^2}{x^6} \qquad (3)$$

with

$$x = \frac{4\pi R n}{\lambda} \sin(\theta/2), \qquad (4)$$

where n is the refractive index of the solvent, m is the relative refractive index of the particles, λ is the wavelength of the light used in vacuo, and I_0 is the incoming light intensity. In the present case, $m \leq 1.14$, $4\pi R/\lambda = 5.5$, and this places the present results in the range [9] where the Rayleigh-Gans-Debye approximation of Eq. (3) should be correct to better than 10%.

I_0 was measured by a photodiode and $I_s(\theta)$ by a Thorn-EMI model RFI/B263 photomultiplier tube operated in the photon counting mode. To determine the relation between measurements of scattered light and measurements of intensity of the incoming laser beam, we calibrated a series of filters using a beam-power meter, used these filters to deliver an attenuated laser beam into the photomultiplier, and measured I_0 and $I_s(0)$ simultaneously. We used this constant conversion factor throughout the experiment to obtain the absolute scattering intensity.

Figure 2 shows a Zimm plot for a typical case. In the Zimm analysis using a Guinier approximation the form factor is approximated as a straight line, but as our particles are large we have to use the full expression for the form factor given in Eq. (3) which results in
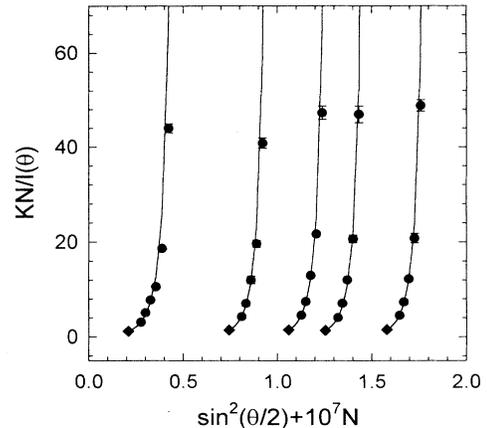
FIG. 2. Measured variation of $\frac{KN}{I(\theta)}$ as a function of colloidal number density plus the scattering angle (Zimm plot) at $|T - T_{\mathrm{coex}}| = 2.80$ K and $c_L = 0.35$. The lines drawm through the data are fits to the full form of the form factor. The extrapolations of these fits to $\theta = 0$ are shown by the solid diamonds.

the fit shown in Fig. 2. This fit allows us to extract the structure factor $S(q)$ from the measured intensities $I(\theta)$ where $q = \frac{4\pi n}{\lambda}\sin(\theta/2)$ is the wave number of the scattering. The problem remains to extrapolate $S(q)$ to determine $S(0)$. In this experiment we have the advantage that we are performing our measurements at extraordinarily small values of the colloidal-particle number density, such small values that reasonable estimates of the q dependence of the structure factor in the region of the first form factor maximum have their first q-dependent terms of order 10^{-5} times the constant term which represents the value of the structure factor at zero wave number. This approximately flat expected structure factor is quite consistent with our observations, as can be seen from Fig. 3 which shows scattering for colloidal particles in pure water at two values of the number density. We do not understand the origin of the simultaneous appearance of the very small q dependence exhibited by the data and the very large N dependence presented below. The effect is, however, very reproducible.

The scattered light intensity at $\theta = 0°$ is then only a function of the number density of the particles and the structure factor $S(0)$, i.e.,

$$I_{\mathrm{ex}}(0) = NS(0)K , \qquad (5)$$

where

$$K = P(0) = \frac{32\pi^4 R^6 |m^2 - 1|^2}{9\lambda^4 r^2}I_0 . \qquad (6)$$

We can also rewrite this equation in a more useful form as

$$\frac{1}{S(0)} = \frac{K}{I_{\mathrm{ex}}(0)}N . \qquad (7)$$

The largest single source of error in the absolute determination of $\frac{1}{S(0)}$ is expected to arise from the use of filters

to determine the absolute ratio $\frac{I_0}{I_{\mathrm{ex}}(0)}$ as discussed above. The uncertainty associated with this procedure could be as large as a factor of 2. A factor of 2 uncertainty in the absolute scale of $S(0)$ could in turn propagate into a factor of 2 uncertainty in the absolute value of the virial coefficient, an uncertainty far smaller than the large effects discussed below. As was mentioned above, the use of the Rayleigh-Gans-Debye approximation to extrapolate to $P(0)$ should produce uncertainties only at the level of 10% or less.

In the dilute colloid limit where the colloidal particles might be expected to approach ideal gas behavior, the density expansion of the zero-wave-number limit of the structure factor can meaningfully be truncated to retain only the first term correcting the ideal gas approximation, the term containing B_2, the second virial coefficient

$$\frac{1}{S(0)} = 1 + \frac{2NB_2}{N_A} , \qquad (8)$$

where N_A is Avogadro's number and

$$B_2(T) = 2\pi N_A \int_0^\infty (1 - e^{-U(r)/kT})r^2 dr, \qquad (9)$$

where r is the distance between the particles and $U(r)$ is the interaction potential.

Figures 4 and 5 show examples of measured values of $\frac{1}{S(0)}$ as a function of colloidal number density. Note that Fig. 4 shows the extrapolation to $\theta = 0$ given in Fig. 2 but at an expanded scale. The slope of these lines determine the second virial coefficient through application of Eq. (8). Also note that the data extrapolate closely to the ideal gas limit $[S(0) = 1]$ at vanishing number density. The slope of the line in Fig. 4 yields the virial coefficient.

Figures 6 and 7 show measured virial coefficients for each of the two different solvent compositions as a function of absolute temperature difference from the coexistence temperature for that solvent composition. In each case the temperature T_a at which aggregation sets in is

FIG. 3. Measured variation of $\frac{1}{S(q)}$ as a function of the wave number at two different number densities ($\bullet$ for $c_{PLS} = 11.6 \times 10^6$ particles/ml and $\square$ for $c_{PLS} = 4.5 \times 10^6$ particles/ml) in pure water. Points for $q \geq 11 \times 10^6$ m^{-1} arise from analysis of intensities which fall in the first minimum of the form factor $P(q)$.
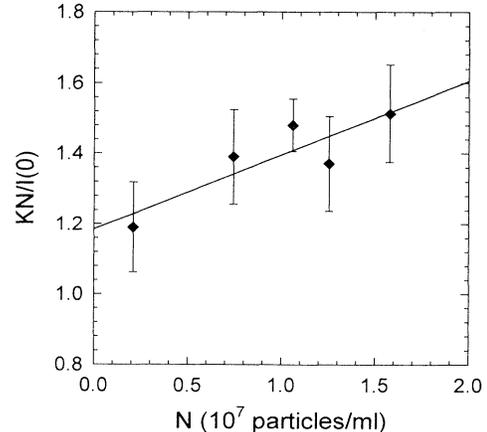
FIG. 4. Measured variation of $\frac{KN}{I(0)}$ as a function of colloidal number density at $|T - T_{\mathrm{coex}}| = 2.80$ K and $c_L = 0.35$.
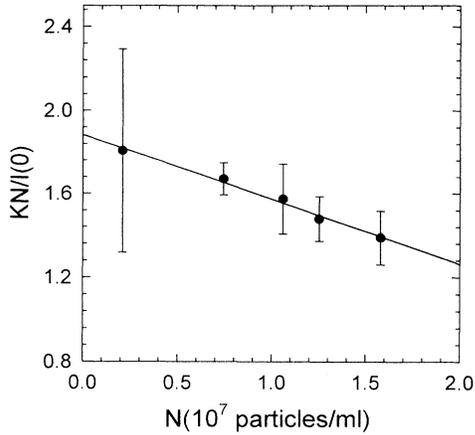
FIG. 5. Measured variation of $\frac{KN}{I(0)}$ as a function of colloidal number density at $|T - T_{\text{coex}}| = 0.48$ K and $c_L = 0.35$.

indicated. In addition, a horizontal line shows the value of the measured virial coefficient for the pure water sample.

Figure 8 shows the solvent-fluctuation correlation length ξ measured with dynamic light scattering for both of our solvent compositions throughout a temperature range which covers the range of our virial coefficient measurement. The figure clearly shows that ξ is, at all temperatures and compositions, much smaller than the particle size and correspondingly gives a static light scattering signal which can be subtracted reliably.

III. DISCUSSION

For each of the two mixed solvent compositions, there is a temperature regime, far from the coexistence curve,
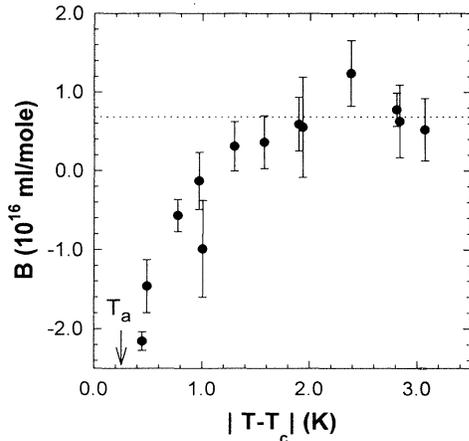
FIG. 6. Temperature dependence of the measured second virial coefficient for $c_L = 0.35$. The horizontal dotted line shows the value of the measured virial coefficient for the pure-water calibration samples. The arrow indicates the temperature T_a at which aggregation sets in.
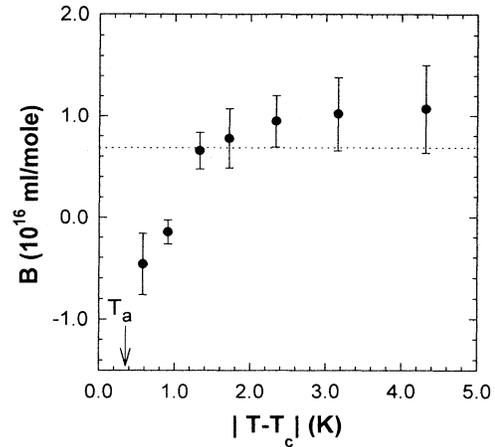
FIG. 7. Temperature dependence of the measured second virial coefficient for $c_L = 0.40$. The horizontal dotted line shows the value of the measured virial coefficient for the pure-water calibration samples. The arrow indicates the temperature T_a at which aggregation sets in.

where the particle interaction is repulsive. This repulsive virial coefficient is very close to that exhibited by the same particles in water for the $c=0.35$ sample and only slightly larger for the $c=0.40$ sample. While the virial coefficient does not change appreciably with temperature far (more than 3 K) from the coexistence curve, as the temperature is moved toward the coexistence curve, each of the mixed solvent samples shows a reduction in the virial coefficient which eventually (approximately 1 K from coexistence for each different composition) changes sign, indicating a net attractive interaction. Because of the obvious limitations coming from the kinetics of aggregation, it was not possible to follow the virial coefficient into the aggregation regime, but in each case, the coefficient was negative and of significant magnitude (compared with the magnitude of the repulsion in pure water) before aggregation set in.
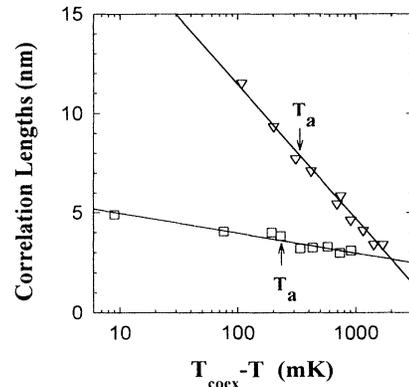
FIG. 8. Variation of the measured correlation length for solvent-composition fluctuations ξ with temperature $|T - T_{\text{coex}}|$, for $c_L = 0.35$ ($\triangledown$) and $c_L = 0.40$ ($\square$). The solid lines through the data are drawn to guide the eye. Also shown is the aggregation temperature T_a for each sample.

In trying to understand the data shown in Figs. 6 and 7, several issues must be considered.

(1) The magnitude of the virial coefficient deep in the repulsive regime is very large. If one naively modeled the particles as hard spheres, this magnitude would correspond to a hard sphere radius of $R = 4.2$ μm, roughly ten times the radius of the particles and comparable to the average interparticle spacing. A hard sphere model with a repulsive-core radius of two particle radii (0.6 μm) should be plausible in this case, since no reasonable estimate of the Debye screening length allows that length to be comparable to the colloidal-particle size. Using the published electrolytic dissociation constant for 2,6-lutidine [11], in our earlier paper we estimated the Debye screening length to be 7-10 nm [5]. Goulian reports evidence for a somewhat larger Debye screening length from measured pH values [12], but it should be noted that it is difficult to remove ions so effectively to raise this length to even as much as 100 nm. This large-apparent radius effect has been measured by Philipse and Vrij in a different system and treated with a speculation that the spheres interact significantly over distances of several radii [13]. Similarly, Thirumalai [14] found a need to set the effective hard sphere radius of colloidal particles to the mean interparticle distance in his calculations in order to explain colloidal crystallization at observed volume fractions.

(2) It is very difficult to explain the large positive virial coefficients observed far from the aggregation temperature. While long range forces are expected in nonequilibrium systems [15], at thermodynamic equilibrium net hydrodynamic interactions are expected to be of short range [16]. Interactions connected with solvent composition fluctuations would not be present in the pure-water sample (which exhibited the same magnitude for the virial coefficient) and, in any case, should not have a range greater than a few solvent correlation lengths (see Fig. 8).

(3) If we restrict our discussion to ignore the long-range repulsion and look for inconsistency with the assumption that the temperature-dependent reduction of the virial coefficient results from solvent-composition fluctuations, it seems reasonable to crudely model the attraction as arising when the surfaces of two particles are separated by only a few solvent correlation lengths ξ. Choosing ten correlation lengths arbitrarily as the maximum range of a plausible overlap of adsorption layers, it is instructive to define a potential

$$U(r) = \begin{cases} \infty & r < 2R \\ -U_0 r & 2R < r < 2R + 10\xi \\ 0 & r > 2R + 10\xi \, . \end{cases} \quad (10)$$

The value of U_0 needed to reduce the virial coefficient by the measured reduction (2×10^{16} ml/mol) in this model is 1.7 kT. Thus no inconsistency is found with assuming a role for adsorption-layer energetics in the aggregation problem.

IV. SUMMARY AND CONCLUSIONS

We have measured the second virial coefficient of very dilute colloidal dispersions of charge-stabilized polystyrene latex spheres in the one-phase region of the mixed solvent 2,6-lutidine plus water. These measurements were made as a function of temperature for two solvent compositions, both of which are richer in 2,6-lutidine than the system's critical composition. The temperature ranges started deep in the one-phase region and approached the coexistence curve but did not penetrate the region of reversible aggregation near the coexistence curve. Far from the aggregation zone, the virial coefficients are large and positive, indicating significant repulsion at much longer range than would be expected from the known particle diameter and any reasonable estimate of the Debye screening length. As the temperature is brought nearer, but definitely not into, the aggregation zone, the virial coefficient plunges through zero to large negative (attractive-interaction) values. It is difficult to model the interactions in terms of known particle properties because the long range of the repulsive interactions is difficult to explain. Crude modeling suggests that the observed changes in the interactions are not inconsistent with a temperature-dependent attraction arising from adsorption-layer energetics operating at distances of a few solvent-fluctuation correlation lengths from the particle surfaces. It is plausible that long-standing work on attractions of walls across mixed solvents [17,18] and recent work on interactions of polymer brushes with mixed solvents [19] could be adapted to shed light on these colloidal-particle interactions if the unexpected repulsive effects can be separated out of the problem.

[1] D. Beysens and D. Estève, Phys. Rev. Lett. **54**, 2123 (1985).

[2] V. Gurfein, F. Perrot, and D. Beysens, Phys. Rev. A **40**, 2543 (1989).

[3] J. S. van Duijneveldt and D. Beysens, J. Chem. Phys.

94, 5222 (1991).

[4] P. D. Gallagher, Ph.D. thesis, University of Pittsburgh, 1991 (unpublished); P. D. Gallagher and J. V. Maher, Phys. Rev. A **46**, 2012 (1992).

[5] P. D. Gallagher, M. L. Kurnaz, and J. V. Maher, Phys.

Rev. A **46**, 7750 (1992).

[6] Interfacial Dynamics Corp., P.O. Box 279, Portland, OR 97207.

[7] Aldrich Chemical Co., Inc., Milwaukee, WI.

[8] H. C. van de Hulst, *Light Scattering by Small Particles* (Dover Publications, New York, 1981).

[9] M. Kerker, *The Scattering of Light and Other Electromagnetic Radiation* (Academic Press, New York, 1969).

[10] P. N. Pusey and R. J. A. Tough, in *Dynamic Light Scattering*, edited by R. Pecora (Plenum Press, New York, 1985).

[11] K. H. Hellwege, A. M. Hellwege, K. Schäfer, and E. Lax, *Eigenschaften der Materie in ihren Aggregatzuständen* (Springer-Verlag, Berlin, 1960).

[12] M. Goulian (private communication).

[13] A. P. Philipse and A. Vrij, J. Chem. Phys. **88**, 6459 (1988).

[14] D. Thirumalai, J. Phys. Chem. **93**, 5637 (1989).

[15] J. F. Brady and G. Bossis, Ann. Rev. Fluid. Mech. **20**, 111 (1988).

[16] A. Shinozaki and Y. Oono, Phys. Rev. E **48**, 2622 (1993).

[17] M. E. Fisher and P. G. de Gennes, C. R. Acad. Sci. (Paris) B **287**, 207 (1978).

[18] H. Nakanishi and M. E. Fisher, Phys. Rev. Lett. **49**, 1565 (1982).

[19] T. C. Tran, A. J. Liu, and P. Pincus, J. Phys. (France) II **4**, 1417 (1994).